Middle East Journal of Science

https://dergipark.org.tr/mejs **MEJS**

e-ISSN:2618-6136

Research Article

ESTIMATION OF NEUTRONS OCCURRING IN THE LINAC ROOM AT DIFFERENT PHOTON ENERGIES

***Taylan TUĞRUL*[1*]**

[1] Department of Radiation Oncology, Medicine Faculty, Van Yüzüncü Yıl University, Van, TURKEY

[*] Corresponding author; taylantugrul@gmail.com

Abstract: *The high-energy photons produced by the Linear accelerator (Linac) induce some nuclear reactions in the materials in the Linac room and Linac head. Neutrons formed as a result of the interaction of photons with materials are called photoneutrons. The aim of the study is to examine the neutron doses formed in the environment for 6 different photon energies. In the study, the components in the Linac head and the Linac chamber are modeled with the help of the Monte Carlo N-Particle (MCNP) program. Then, the flux and dose of photoneutrons formed at 8 different points as a result of 6 different photon energies obtained from the Linac head were measured. as can be seen from the results, as the photon energy used in the Linac increases, the resulting dose, and flux of photoneutron increase. It can be understood from the results that the amount of neutron dose to be received by the organs in the treatment field may be higher than the other organs. Especially in the treatments where the patient is lying in the prone position, there may be a possibility of neutrons reaching the patient spinal cord. Since photoneutrons with high radiobiological ability may pose a risk of secondary cancer for patients, the photon energy chosen for patient treatments should be chosen appropriately and the use of unnecessary high photon energy should be avoided.*

Keywords*: Photoneutron, MCNP, Linac, Neutron Flux.*

Received: October 10, 2021 Accepted: December 25, 2021

1. Introduction

Although there are many methods used for cancer treatment, the method of radiotherapy utilizing photons and electrons is the most commonly used technique [1]. Electron energies from 6 MeV to 25 MeV can be generated in Linear accelerator (Linac) devices, which have been used in radiotherapy [2,3]. Because tungsten is a good material used to reduce the energy of photons, the important components of Linac consist of tungsten. The primary collimator, jaws, and multi-leaf collimator (MLC), which are possessed in Linac, are these components. The flattening filter affecting the photon beam is usually made of steel [4].

Although the use of high-energy photons is a good method for cancer treatment, it has a downside. During the radiotherapy treatment applied to the patient, some nuclear reactions that can generate neutrons occur in the Linac room due to the high energy radiation obtained in the Linac devices [2,4,5,6]. The photon energy directly affects neutron production [4].

The photons created by the Linac cause undesirable neutron formation in the environment after a certain threshold value [7,8,9,10]. These undesirable neutrons, which are demonstrated a high linear

energy transfer (LET) ability, indicate secondary cancer risk for the patients and can ever reach staff outside the room [6,11,12,13].

The atomic number (Z) of the environment in which the radiation is emitted directly affects the threshold value of the photon energy for the formation of nuclear reactions. While this threshold value is 7 MeV for the nuclear reaction that may occur in materials with a high Z value such as tungsten, this value is 16 MeV for oxygen with a low Z value [14,15]. The process from primary electron generation to the transport of all radiation and all nuclear reactions that may occur can be modeled with the Monte Carlo (MC) method [14].

The neutron created by the photon is called photoneutron. The high-density head components of the Linac are associated with the photoneutrons produced. In addition, these photoneutrons can also be produced from the wall concrete in the room of Linac and the patient body [12,16,17,18,19]. The main cause of the photoneutrons formation is nuclear reactions between tungsten and photon. Photoneutrons are also formed in the environment due to other materials (flatting filter, source thickness, etc.) but they are neglected because their ratio is low [6]. It has been stated in previous studies that most of the neutrons formed (87%) are due to tungsten components [12,20].

The photoneutrons formed in the Linac head and Linac room are obtained as direct reaction neutrons (knock-on) and evaporation neutrons [4]. When photons interact with a nucleus, their energy is dispersed among nucleons. When a neutron near the nucleus surface achieves enough energy, that neutron is emitted from the nucleus as an evaporation neutron. Photoneutron, known as a knock-on neutron, occurs when the photon gives all of its energy to a single neutron. In addition, this neutron spreads mainly in the direction of the incoming photon [2,6,21]. Photoneutrons produced by nuclear reactions as a result of the use of Linac is roughly 100 to 200 times larger than electron-neutron production, so studies have focused on photoneutrons [6,8,19].

This study aims to examine the neutron flux and neutron dose that can occur in the environment at different photon energies obtained from Linac. Measurement results were obtained at eight different points.

2. Materials and Methods

In the study, the simple model of the head of Linac was simulated by MCNPX2.6 MC code [22]. The Monte Carlo N-Particle (MCNP) code is a common code for examining neutron, photon, and electron transport. A protective shield made of lead covering the head of the Linac is also included in the modeling. The simulations were implemented for six different photon energies and 10x10 cm^2 field sizes. In the modeling, detectors in the eight different points were defined to measure neutrons. The detectors were employed to calculate the flux (Particle x cm^{-2} x s^{-1}) and neutron dose (mrem/hour). Some measurement points were selected from regions that may be critical to the patient. If we define the target position as (0,0,0) on the x, y and z axes, detector positions; (0,0,-90) for Point 1, (0,0,-50) for Point 2, (-40,0,-100) for Point 3, (-80,0,-100) for Point 4, (0,-40,-100) for Point 5, (0,-80,-100) for Point 6, (-240,-180, -100) for Point 7 and (-145,-400,-100) for Point 8. The created simulation is shown in Figure 1 and Figure 2.

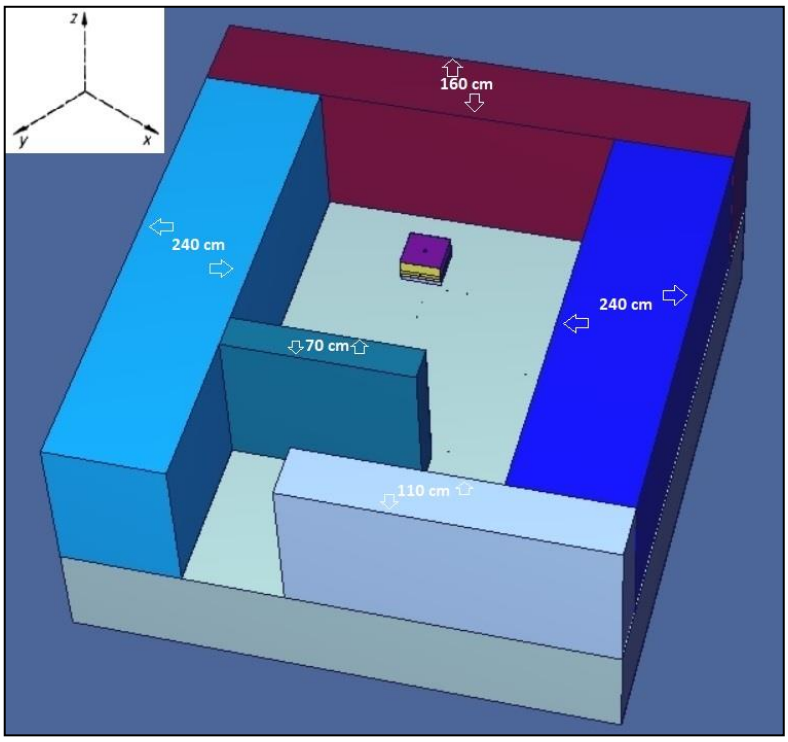

Figure 1. Simulation image of Linac room and Linac head created in MCNP

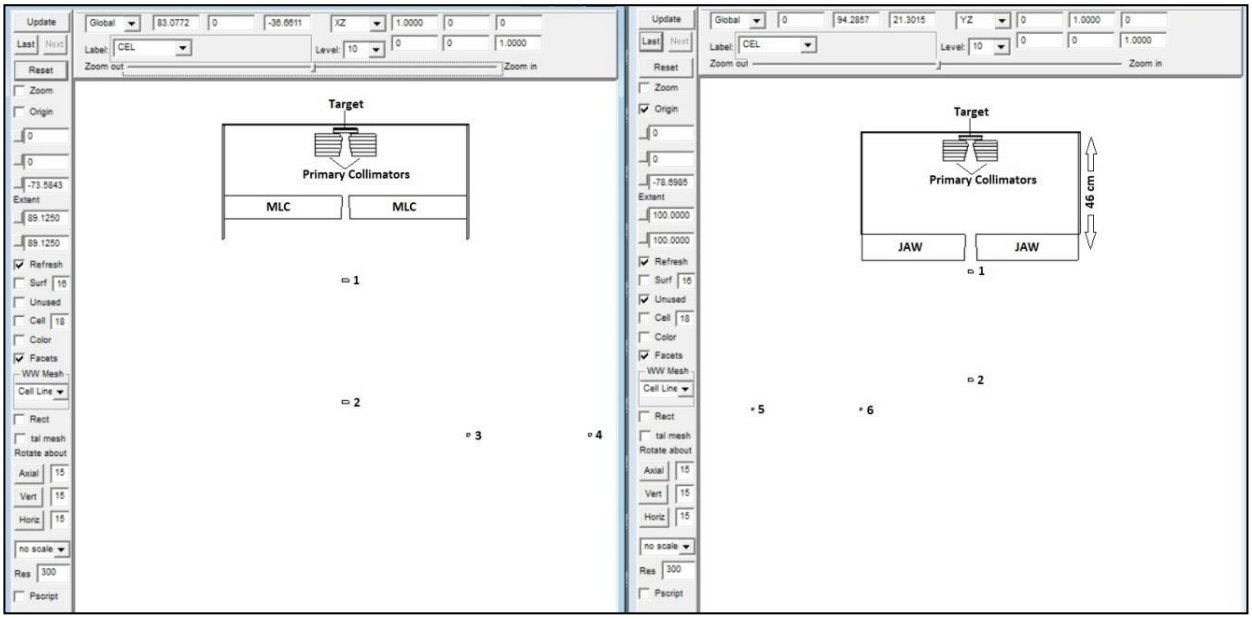

Figure 2. Simulation image of some detectors and Linac head created in MCNP

The geometric structure of the Linac room, which includes all its components and thickness, has been taken into account. In addition, the target, flattening filter, primary collimator, jaws, and MLC components of the Linac head are also considered. Agosteo et al. and Carinou et al. have pointed out that there was no significant difference in comparing a simple MC model and a detailed MC model [23,24]. The walls of the Linac room were simulated with a 2.35 gr/cm3 density concrete type containing 50.0% O, 31.5% Si, 8.3% Ca, 4.8% Al, 1.9% K, 1.7% Na, 1.2% Fe and 0.6% H [2,25].

In MCNP, the F5 tally was used to measure the flux and neutron dose. It was utilized the variance reduction technique was to reduce the computation time and focus on the desired result in modeling. In MCNP, the F5 tally was modified with the help of DE/DF dose factors, and the dose values at the desired points were obtained as "mrem/hour" [22,26]. The results were acquired using e/ɣ/n mode in MCNP and run for 109 histories. The statistical uncertainties obtained for all results were below 1%.

3. Results

As a result of 6 different photon energies produced in the Linac head, the flux and dose of photoneutrons occurring in different positions of the Linac chamber were investigated. Photoneutrons formed in the Linac room are made up of knock-on and evaporation contributions. Contributions from other reactions are quite small [6]. Some of the locations where photoneutrons are measured have been attempted to be chosen similarly to places where the patient's surface may be exposed during treatment. The results at the points where flux and dose were measured for the photoneutron are shown in Table 1 and Table 2.

Table 1. The obtained flux values for 6 different photon energies.

	Flux (Particle x cm^{-2} x s^{-1})							
	Point 1	**Point 2**	**Point 3**	**Point 4**	**Point 5**	**Point 6**	**Point 7**	**Point 8**
6 MV	N/A	N/A	N/A	N/A	N/A	N/A	N/A	N/A
8 MV	1,23E-08	5,27E-08	7,62E-10	5,52E-09	2,25E-09	4,80E-09	2,17E-09	6,13E-10
10 MV	6,08E-07	5,66E-06	6,04E-08	1,80E-07	1,33E-07	1,76E-07	7,34E-08	2,01E-08
12 MV	3,55E-06	2,15E-05	3,54E-07	9,66E-07	6,18E-07	9,90E-07	3,85E-07	1,05E-07
15 MV	2,18E-05	1,24E-04	1,51E-06	5,88E-06	3,02E-06	6,55E-06	2,32E-06	6,15E-07
18 MV	7,55E-05	4,14E-04	4,41E-06	1,99E-05	8,78E-06	2,36E-05	7,79E-06	2,03E-06

Table 2. The obtained neutron dose values for 6 different photon energies.

	Dose (mrem/hour)							
	Point 1	**Point 2**	**Point 3**	**Point 4**	**Point 5**	**Point 6**	**Point 7**	**Point 8**
6 MV	N/A	N/A	N/A	N/A	N/A	N/A	N/A	N/A
8 MV	1,14E-12	4,73E-12	4,55E-14	3,93E-13	1,68E-13	3,54E-13	1,51E-13	4,34E-14
10 MV	6,88E-11	6,88E-10	6,81E-12	1,94E-11	1,50E-11	1,92E-11	7,89E-12	2,16E-12
12 MV	3,96E-10	2,40E-09	3,91E-11	1,05E-10	7,10E-11	1,08E-10	4,21E-11	1,16E-11
15 MV	2,55E-09	1,46E-08	1,76E-10	6,81E-10	3,53E-10	7,57E-10	2,68E-10	7,11E-11
18 MV	9,18E-09	4,96E-08	5,26E-10	2,41E-09	1,05E-09	2,86E-09	9,38E-10	2,44E-10

Khaledi et al. stated that the threshold value of tungsten for the formation of photoneutrons is 7.42 MeV in their study [12]. In our study, we also did not observe flux and neutron dose values for the photoneutron at 6 MV photon energy.

As expected, as the photon energy increased, the photoneutrons formed in the medium also increased. We obtained the highest photoneutron value at point 2, 50 cm from the source. The second highest value was measured at 90 cm (Source-skin distance (SSD)=90) from the source. As the measurement points moved away from the central photon axis, the photoneutron flux and dose began to decrease. This is a result of the same trend as other studies [2,21,27]. It can be understood from this result that the amount of neutron dose to be received by the organs in the treatment field may be higher than the other organs. As seen in Table 2, when the photoneutrons formed at a distance of SSD=90 cm are examined, there is an approximately 8 thousand-fold difference between 8 MV and 18 MV.

The lowest flux and dose values were measured at the farthest point from the source. The photoneutron dose and flux values at Points 3-5 and 4-6, which are equidistant from the source, were found to be close to each other. The differences between them can be attributed to the axis positions of the MLC and jaws. Photoneutrons measured in the study also include contaminated neutrons produced by the interaction of photons with concrete.

4. Conclusion

Since photoneutrons, which are harmful to normal tissues, formed during radiotherapy treatment may lead to the risk of secondary cancer, their behavior in the environment should be carefully examined. As can be seen from the results, as the photon energy used in the Linac devices increases, the resulting photoneutron dose, and flux increase. Photoneutrons reaching critical organs may cause some complications and secondary cancer risk in the patient. Furthermore, photoneutrons can reach the spinal cord, especially when the patient is in a prone position. Photon energy selected for patient treatments should be chosen appropriately, unnecessary high photon energy use should be avoided.

Ethical statement

Ethical approval is not required for this study, as no patient or animal data were used in the study.

Conflict of interest

The authors must notify any conflicts of interest.

Authors' Contributions

T. T: Measurement, Literature review, Simulation, Modelling, Writing - Original draft preparation
The author reads and approved the final manuscript.

References

[1] Mesbahi, A., Keshtkar, A., Mohammadi, E., Mohammadzadeh, M., "Effect of wedge filter and field size on photoneutron dose equivalent for an 18MV photon beam of a medical linear accelerator", *Applied Radiation and Isotopes*, 68, 84–89, 2010.

[2] Khabaz, R., Boodaghi, R., Benam, M.R., Zanganeh, V., "Estimation of photoneutron dosimetric characteristics in tissues/organs using an improved simple model of linac head", *Applied Radiation and Isotopes*, 133, 88–94, 2018.

[3] Vega-Carrillo, H.R., Hernandez-Almaraz, B., Hernandez-Da´vila, V.M., Ortiz-Hernandez, A., "Neutron spectrum and doses in an 18MV LINAC", *Journal of Radioanalytical and Nuclear Chemistry*, 283, 261–265, 2009.

[4] Khabaz, R., "Effect of each component of a LINAC therapy head on neutron and photon Spectra", *Applied Radiation and Isotopes*, 139, 40-45, 2018.

[5] Naseri, A., Mesbahi, A., "A review on photoneutrons characteristics in radiation therapy with high-energy photon beams", *Reports of Practical Oncology and Radiotherapy*, 15, 138–144, 2010.

[6] Vega-Carrillo, H.R., Martı´nez-Ovalle, S.A., Lallena, A.M., Mercado, G.A., Benites- Rengifo, J.L., "Neutron and photon spectra in LINACs", *Applied Radiation and Isotopes*, 71, 75–80, 2012.

[7] Followill, D.S., Nüsslin, F., Orton, C.G., "IMRT should not be administered at photon energies greater than 10 MV", *Medical Physics*, 34, 1877–1879, 2007.

[8] Lin, J.P., Chu, T.C., Lin, S.Y., Liu, M.T., "The measurement of photoneutrons in the vicinity of a Siemens Primus linear accelerator", *Applied Radiation and Isotopes*, 55, 315–321, 2001.

[9] Vega-Carrillo, H.R., Baltazar-Raigosa, A., "Photoneutron spectra around an 18 MV LINAC", *Journal of Radioanalytical and Nuclear Chemistry*, 287, 323–327, 2011.

[10] Zanini, A., Durisi, E., Fasolo, F., Ongaro, C., Visca, L., Nastasi, U., Burn, K.W., Scielzo, G., Adler, J.O., Annand, J.R.M., Rosner, G., "Monte Carlo simulation of the photoneutron field in linac radiotherapy treatments with different collimation systems", *Physics in Medicine and Biology*, 49, 571-582, 2004.

[11] Benites-Rengifo, J.L., Vega-Carrillo, H.R., "Neutron Dosimetry in Solid Water Phantom", AIP Conference Proceedings 1626, 114-116, 2014.

[12] Khaledi, N., Dabaghi, M., Sardari, D., Samiei, F., Ahmadabad, F.G., Jahanfarnia, G., Saadi, M.K., Wang, X., "Investigation of photoneutron production by Siemens artiste linac: A Monte Carlo Study", *Radiation Physics and Chemistry*, 153, 98–103, 2018

[13] Agosteo, S., FoglioPara, A., "Energy and spatial dependence of neutron fluxes in radiotherapy rooms for a simple dose estimate method", *Nuclear Instruments and Methods in Physics Research Section B: Beam Interactions with Materials and Atoms*, 93, 362–369, 1994.

[14] Sumini, M., Isolan, L., Cucchi, G., Sghedoni, R., Iori, M., "A Monte Carlo model for photoneutron generation by a medical LINAC", *Radiation Physics and Chemistry*, 140, 345–348, 2017.

[15] Burn, K.W., Ongaro, C., Photoneutron production and dose evaluation in medical accelerators, Cern Libraries, Geneva, 2002.

[16] d'Errico, F., Nath, R., Tana, L., Curzio, G., Alberts, W.G., "In-phantom dosimetry and spectrometry of photoneutrons from an 18 MV linear accelerator", *Medical Physics*, 25, 1717–1724, 1998.

[17] Hall, E.J., Martin, S.G., Almols, H., Hei, T.K., "Photoneutrons from medical linac accelerators radiobiological measurements and risk estimates", *International Journal of Radiation Oncology - Biology - Physics*, 33, 225–230, 1995.

[18] IAEA, Handbook on Photonuclear Data for Applications. Cross-Sections and Spectra, International Atomic Energy Agency IAEA-TECDOC-1178, Vienna, 2000.

[19] Martinez-Ovalle, S.A., Barquero, R., Gomez-Ros, J.M., Lallena, A.M., "Neutron dose equivalent and neutron spectra in tissue for clinical linacs operating at 15, 18 and 20 MV", *Radiation Protection Dosimetry*, 147, 498–511, 2011.

[20] Pena, J., Franco, L., Gomez, F., Iglesias, A., Pardo, J., Pombar, M., "Monte Carlo study of Siemens PRIMUS photoneutron production", *Physics in Medicine and Biology*, 50, 5921-5933, 2005.

[21] Mohammadi, N., Miri-Hakimabad, S.H., Rafat-Motavalli, L., "A monte carlo study for photoneutron dose estimation around the high-energy linacs", *Journal of Biomedical Physics & Engineering*, 4, 127–139, 2014.

[22] MCNP Version 2.6.0, MCNPX USER'S MANUAL. Los Alamos National Laboratory, USA, 2008.

[23] Agosteo, S., FoglioPara, A., Maggioni, B., Sangiust, V., Terrani, S., Borasi, G., "Radiation transport in a radiotherapy room", *Health Physics*, 68, 27–34, 1995.

[24] Carinou, E., Kamenopoulou, V., Stamatelatos, I.E., "Evaluation of neutron dose in the maze of medical electron accelerators", *Medical Physics*, 26, 2520–2525, 1999.

[25] Khabaz, R., "Analysis of neutron scattering components inside a room with concrete walls", *Applied Radiation and Isotopes*, 95, 1–7, 2015.

[26] White, D.R, Griffith, R.V., Wilson I.J., Photon, Electron, Proton, and Neutron Interaction Data for Body Tissues ICRU Report 46, International Committee on Radiation Units and Measurements, USA, 1992.

[27] Ghiasi, H., Mesbahi, A., "Monte Carlo characterization of photoneutrons in the radiation therapy with high-energy photons: a comparison between simplified and full Monte Carlo models", *Iranian journal of radiation research*, 8, 187–193, 2010.